Dynamic directed interictal connectivity in left and right temporal lobe epilepsy

*Ana Coito, *Gijs Plomp, *Mélanie Genetti, †Eugenio Abela, †Roland Wiest, ‡Margitta Seeck, *Christoph M. Michel, and *† Serge Vulliemoz

Ana Coito is a PhD candidate in the Functional Brain Mapping Lab at the University of Geneva, Switzerland.

SUMMARY

Objective: There is increasing evidence that epileptic activity involves widespread brain networks rather than single sources and that these networks contribute to interictal brain dysfunction. We investigated the fast-varying behavior of epileptic networks during interictal spikes in right and left temporal lobe epilepsy (RTLE and LTLE) at a whole-brain scale using directed connectivity.

Methods: In 16 patients, 8 with LTLE and 8 with RTLE, we estimated the electrical source activity in 82 cortical regions of interest (ROIs) using high-density electroencephalography (EEG), individual head models, and a distributed linear inverse solution. A multivariate, time-varying, and frequency-resolved Granger-causal modeling (weighted Partial Directed Coherence) was applied to the source signal of all ROIs. A nonparametric statistical test assessed differences between spike and baseline epochs. Connectivity results between RTLE and LTLE were compared between RTLE and LTLE and with neuropsychological impairments.

Results: Ipsilateral anterior temporal structures were identified as key drivers for both groups, concordant with the epileptogenic zone estimated invasively. We observed an increase in outflow from the key driver already before the spike. There were also important temporal and extratemporal ipsilateral drivers in both conditions, and contralateral only in RTLE. A different network pattern between LTLE and RTLE was found: in RTLE there was a much more prominent ipsilateral to contralateral pattern than in LTLE. Half of the RTLE patients but none of the LTLE patients had neuropsychological deficits consistent with contralateral temporal lobe dysfunction, suggesting a relationship between connectivity changes and cognitive deficits.

Significance: The different patterns of time-varying connectivity in LTLE and RTLE suggest that they are not symmetrical entities, in line with our neuropsychological results. The highest outflow region was concordant with invasive validation of the epileptogenic zone. This enhanced characterization of dynamic connectivity patterns could better explain cognitive deficits and help the management of epilepsy surgery candidates.

KEY WORDS: Temporal lobe epilepsy, Directed connectivity, Weighted Partial Directed Coherence, High-density EEG, Electrical source imaging.

Focal epilepsy is increasingly recognized as a dysfunction of large-scale brain networks rather than one circumscribed brain region. The organization of these brain networks and their dynamics is key to understanding the onset and spread of epileptic activity, the clinical expression of seizures, and cognitive impairment in focal epilepsies.[1]

Temporal lobe epilepsy (TLE) is the most common type of pharmacoresistant epilepsy in adults, frequently successfully

treated by surgery, although long-term relapses in up to 58% of cases[2] suggest insufficient network disruption.

Cognitive impairments in unilateral TLE frequently involve the contralateral temporal lobe and frontal lobes,[3,4] including difficulties in problem solving, working memory, and executive functions.[3,4] These findings support the dysfunction of remote brain areas in TLE. Indeed, studies in TLE reported altered functional connectivity between brain regions using invasive and noninvasive electrophysiology, functional magnetic resonance imaging (MRI), isotopic imaging,[5–9] and structural abnormalities (cortical thickness, diffusion tractography),[10] which expanded beyond the affected temporal lobe, ipsilaterally and contralaterally. Moreover, interictal spikes can transiently worsen these deficits,[11] and thus, describing large-scale brain interactions with high temporal resolution is important for understanding the epileptic networks dynamics.

There is evidence that networks involved in left TLE (LTLE) and right TLE (RTLE) are not symmetrical. Verbal memory is more lateralized to the language-dominant hemisphere, whereas nonverbal memory is lateralized (but to a lesser extent) to the other hemisphere. Postoperative verbal memory deficits are more consistently reported by LTLE patients, also supporting the possibility of a different network organization for both memory modalities.[12] Brain network imaging concordantly showed different patterns of contralateral damage in both LTLE and RTLE.[13,14]

Functional connectivity measures the nondirectional statistical dependency between different signals. Effective or directed connectivity, however, investigates directional relationships (causal influence). This can be investigated using data-driven techniques based on Granger-causal modeling.[15–18] Such measures have been successfully applied to intracranial EEG recordings of patients with epilepsy during interictal spikes[9] or seizures.[6,7] A magnetoencephalography (MEG) connectivity study in focal epilepsies showed a good concordance between regions of strongest outflow and resection areas.[5] However, the time-varying pattern of interictal connectivity has not yet been investigated noninvasively. This is an important issue given that spikes are transient highly nonstationary events with fast propagation and their contribution to cognitive impairment is poorly understood.

In this study, we investigated large-scale brain connectivity changes during interictal spikes in RTLE and LTLE, using Granger-causal modeling (time-varying weighted Partial Directed Coherence [PDC])[15–17] applied to EEG source signals. We hypothesized that (1) the connectivity of the regions involved in the generation and propagation of interictal epileptic activity is transiently altered during spikes; (2) the outflow of neural information is concordant with the localization of the epileptogenic zone; (3) the network spatial pattern is different in LTLE and RTLE; (4) neuro-

psychological impairment is concordant with the network patterns.

METHODS

The analysis strategy is summarized in Figure 1.

Patients

We searched the database of the presurgical evaluation centers in the epilepsy unit of the Geneva University Hospital and the epilepsy center of the University Hospital in Bern for patients that fulfilled the following criteria: (1) drug-resistant anteromedial temporal lobe epilepsy (epileptogenic zone involving anterior temporal medial structures and the temporal pole); (2) unilateral anteromedial temporal lobe focus confirmed by intracranial recordings or successful anterior temporal lobectomy (outcome Engel's class I or II); (3) high-resolution EEG recording (96–256 channels) with unilateral spikes corresponding to the site of the focus. We pragmatically considered only recordings with at least five spikes. Sixteen patients (mean age 32 ± 14.5; 12 male) were identified (eight RTLE and eight LTLE) (Table 1). All patients except for one RTLE patient (P11) were right-handed. For comparison of clinical data between LTLE and RTLE, a nonparametric Mann-Whitney-Wilcoxon test was used.

Presurgical neuropsychological assessments were reviewed retrospectively by a neuropsychologist blind to connectivity results (M.G.). This comprehensive routine clinical testing was not specifically designed for this study and did not include the same tests across patients. Consequently, we constructed a semi-quantitative scale of cognitive deficits associated with different brain regions. For this purpose, we divided the brain into left/right, superior/middle/inferior/medial temporal and dorsolateral/frontal orbital cortex (see Table S1). We then characterized each region according to the results of these clinical tests using Swiss-specific norm values (no deficit, mild deficit z-score between -2.33 and -1.65, severe deficit z-score below -2.34).

The study was approved by both local ethical committees and patients gave written informed consent.

EEG acquisition and preprocessing

At least 30 min of awake, eyes-closed, resting state, high-resolution EEG was recorded for each patient. Sampling rates ranged between 250 and 1,000 Hz and data were down sampled off line to 250 Hz for consistency and to reduce computation duration. Isolated interictal epileptiform discharges (spikes) free of major artifacts were selected by a neurologist with EEG expertise (S.V.). Epochs of 460 msec around the maximal negativity of each interictal spike (260 msec before and 200 msec after the spike) were selected. To avoid contamination of the epochs
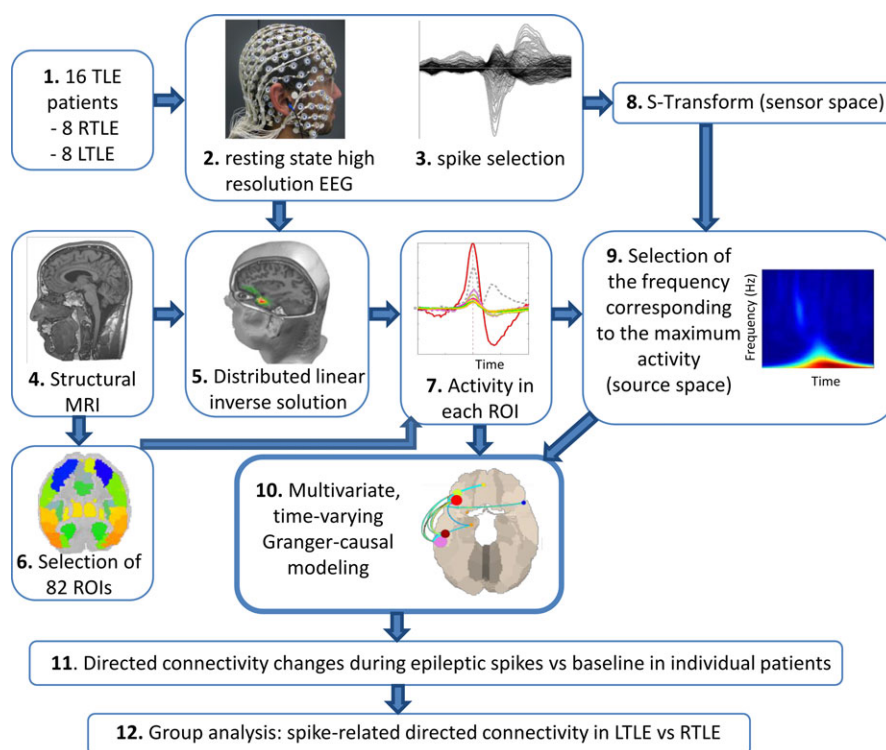
Figure 1.
Summary of the analysis strategy.
Epilepsia © ILAE

Patient	Gender	Age (year)	Age of epilepsy onset (year)	Focus side	Interictal spikes ipsilateral %	Seizure frequency (N/month)	Structural epileptogenic lesion on MRI	Surgery outcome (Engel class)	Intracranial EEG
P1	M	18	8	Left	70	20	HS	I	No
P2	M	15	1.2	Left	100	6	MTD	I	No
P3	M	18	13	Left	85	10	Normal	I	Yes
P4	M	35	27	Left	100	8	HS	I	No
P5	M	53	2.5	Left	100	10	HS	I	No
P6	M	33	15	Left	73	2.5	Normal	II	Yes
P7	F	29	26	Left	100	3	Tumor	I	No
P8	F	15	9	Left	100	3.5	Tumor	I	No
P9	F	56	3	Right	100	5	HS	I	No
P10	M	16	11	Right	100	15	HS	I	Yes
P11	M	40	22	Right	95	30	Normal	not operated	Yes
P12	M	20	3	Right	100	20	Tumor	I	No
P13	M	27	5	Right	100	3	HS	I	No
P14	M	37	20	Right	100	150	HS	I	No
P15	F	55	4	Right	100	2	HS	I	No
P16	M	50	2.5	Right	100	4	HS	I	No

Table 1. Patient demographics and clinical data

HS, hippocampus sclerosis; MTD, medial temporal dysplasia.

by a previous spike, only spikes occurring at least 1 s after the previous interictal discharge peak were included. In total, 121 interictal spikes were selected in the LTLE group and 126 in the RTLE group. For each patient, the same number of artifact-free baseline epochs (i.e., without spikes) was also selected with the same duration and arousal state. Spike and baseline epochs were filtered between 1 and 100 Hz.

Regional electrical source imaging (ESI)

The forward model consisted in a simplified realistic head model with consideration of skull thickness (Locally Spheri-

cal Model with Anatomical Constraints [LSMAC][19,20]). From the segmented individual T_1-weighted MRI ($1 \times 1 \times 1$ mm^3), around 5,000 solution points were distributed equally in the gray matter, which represented the solution space. This head model produces localization precisions similar to the realistic Boundary Element Model (BEM) and Finite Element Model (FEM).[19] A linear distributed inverse solution with biophysical constraints was used to calculate the three-dimensional (3D) current density distribution (Local Auto-Regressive Averages [LAURA]).[21] The inverse solution was first applied to the average interictal spike of each patient to confirm the localization, and then a grand average was performed for both groups. For the subsequent connectivity analysis, the inverse solution was applied to each individual spike and baseline epoch.

The brain was parcelled into 82 regions of interest (ROIs) using the automated anatomic labeling (AAL) digital atlas[22] coregistered with each individual brain using the inverse segmentation matrix obtained in SPM8 (www.fil.ion.ucl.ac.uk/spm). The source activity of the solution point closest to the geometric center of each ROI (centroid) was considered as the representative source activity of the ROI (centroids). To account for the changing tridimensional orientation of the source dipoles, these were projected at each time point on the predominant dipole direction of each ROI to obtain scalar values of the current density.

Time-varying weighted Partial Directed Coherence

For each patient, we selected the ROI with the highest source activity during the spike (Fig. 1.7). We calculated the time–frequency distribution of the power spectral density (PSD) using the S-transform (ST)[23] and selected the frequency with the maximum power, considering that the information transfer would be most relevant at that frequency.[6,16] The PDC results (for both spike and baseline epochs, see below) were analyzed only at this frequency. To determine the PSD for each voxel in the inverse space, ST was computed for each scalp electrode (Fig. 1.8), and source estimation was then applied to this frequency–domain complex data[24] (Fig. 1.9). The mean PSD for each patient was computed and normalized (0–1) across regions, time, and frequencies (1–100 Hz) by subtracting the minimum power and dividing by the range.

Time-varying PDC estimates directed interactions between pairs of signals in the time and frequency domain using adaptive multivariate autoregressive models (AMVAR) of an appropriate order.[15,17] We estimated the time-varying AMVAR parameters by means of a recursive least squares (RLS) algorithm.[17,25] Because we used time-varying autoregressive models, which are designed to model nonstationary signals, we refrained from removing the spike-ensemble average. PDC has been successfully applied in simulation studies,[26] animal data,[16] and human intracranial EEG spikes.[27] We used a model order of 15 (i.e., 60 msec) following previous work.[17] PDC values

were scaled (in the same way as the ST) and multiplied by the spectral power (weighted PDC, wPDC).[6,16] A full description of the wPDC method used can be found in previous work.[16] For each patient, a four-dimensional (4D) connectivity matrix (ROIs $\times$ ROIs $\times$ time points $\times$ epochs) represented the flow from one ROI to another at a certain time and for each epoch.

The summed outflow for a given ROI and time point was defined as the sum of wPDC values from that ROI to all others ROIs at that time point. It reflects the importance of a ROI for the network: ROIs with high summed outflow strongly drive activity of other ROIs.

For each patient, the summed outflow of each region at each time point of the spike epoch was compared to the temporal average of each baseline epoch with a nonparametric test (Mann-Whitney-Wilcoxon, $p < 0.05$). The summed outflow across the rising phase of the spike was taken to represent the network involved in the generation of interictal spikes and early propagation in accordance with earlier work.[28]

We applied two criteria to identify key drivers: (1) ROIs with high summed outflow (>50% of the maximum) during this rising phase and statistically significant in at least half of the patients (4/8) and (2) ROIs statistically significant in at least 7/8 of the patients (independent of the amount of outflow). Group-level analysis was performed by taking the averaged summed outflow across the spike rising phase in the regions that showed a statistically significance.

To investigate the connectivity from these regions (network pattern), the flow from these selected ROIs to all others was then compared to the baseline epochs, for each patient. For each group, we considered connections from one ROI to the other that were significant in at least half of the patients. Group analysis for investigation of the connections from the chosen ROIs was performed in the same way as described for the summed outflow. A chi-square test between LTLE and RTLE was performed in each selected ROI.

To assess whether one group had more summed outflow ipsilateral or contralateral to the epileptic source, we defined a laterality index as:

$$\text{Laterality} = \frac{\text{sum}(S_{ips}) - \text{sum}(S_{cont})}{\text{sum}(S_{whole})}$$

where S_{ips}, S_{cont}, and S_{whole} are, respectively, the total summed outflow of all ipsilateral regions, contralateral regions, and the whole brain. Mann-Whitney-Wilcoxon test ($p < 0.05$) was performed to compare laterality in LTLE versus RTLE. A multivariate linear regression was carried out, considering laterality measure as dependent variable and the age of onset and the duration of the disease as independent variables.

EEG and ESI analysis were carried out using the freely available software *Cartool* (brainmapping.unige.ch/cartool)

and *Matlab* (MATLAB and Statistics Toolbox Release 2012b, The MathWorks, Inc., Natick, Massachusetts, United States). For some figures, we used a modified version of the e-connectome toolbox.[29]

RESULTS

Clinical data

Clinical characteristics (age, age at epilepsy onset, disease duration, presence of ictal loss of contact, number of seizures per month, evolution toward tonic–clonic generalization, and percentage of ipsilateral interictal spikes) were not significantly different between groups (Table 1).

Electrical Source Imaging

The number of spikes analyzed for each individual ranged from 5 to 20 per patient in both groups. In all patients, the ESI maximum was in the anteromedial temporal lobe (illustrative case in Fig. 2C). The parceling into ROIs showed that the region with maximum activity during the spike was the medial temporal pole in both groups (Fig. 2D, E). The frequency of maximum activity at the time of the spike was 6.4 ± 1.9 Hz for the LTLE group and 6.8 ± 1.8 Hz for the RTLE group.

In LTLE, the ROIs with highest activity were all localized ipsilateral to the epileptic focus (Fig. 2D). In the RTLE, the ROIs displaying the highest activity (besides the medial temporal pole) were in both ipsilateral and contralateral hemispheres (Fig. 2E).

Time-varying directed connectivity

Summed outflow

The key drivers showed an ipsilateral predominance in LTLE (Fig. 3A) but a more bilateral pattern in RTLE (Fig. 3B). The main drivers in LTLE were the ipsilateral medial temporal pole, medial temporal, inferior temporal, and inferior frontal orbital regions. In RTLE, the ipsilateral regions with largest summed outflow were the medial temporal pole and the gyrus rectus, and the contralateral regions were the medial temporal pole and the inferior frontal orbital region. The ipsilateral hippocampus and amygdala showed also a significant difference from baseline in 87.5% (7/8) of the patients in both groups, although with low absolute summed outflow. In the contralateral hippocampus and amygdala, the outflow was significantly different from baseline in >50% in RTLE but not significant in LTLE. The drivers were not limited to the temporal lobe but involved frontal regions as well: almost exclusively ipsilateral frontal regions in the LTLE group and bilateral regions in the RTLE group. Indeed, the inferior frontal orbital region (ipsilateral in LTLE and bilateral in RTLE) was one of the drivers with highest summed outflow.

We restricted the subsequent analysis to the identified key drivers: ipsilateral medial temporal pole, superior temporal pole, inferior frontal orbital, gyrus rectus, hippocampus, parahippocampus, amygdala, medial temporal gyrus, inferior temporal gyrus, and contralateral medial temporal pole, inferior frontal orbital gyrus, and superior temporal pole.

The summed outflow from the ipsilateral inferior temporal gyrus was more often significant in LTLE than RTLE ($p < 0.001$). On the other hand, the contralateral inferior frontal orbital gyrus and superior temporal pole were more often recruited in RTLE versus LTLE (respectively, $p = 0.02$; $p = 0.007$). The summed outflow in the ipsilateral medial temporal gyrus and inferior temporal gyrus was larger in LTLE than RTLE (Mann-Whitney-Wilcoxon, $p = 0.038$ and $p = 0.0023$, respectively) and the contralateral superior temporal pole was larger in RTLE than LTLE ($p = 0.025$).

Network dynamics

For the 12 key drivers of each group, the rise in summed outflow occurred predominantly before the spike peak (Fig. 3C,D). In both groups, key drivers became statistically significant approximately 100 msec before the spike peak, and the ipsilateral medial temporal pole was the first region with significant outflow. In the LTLE group, it was rapidly followed by the ipsilateral medial temporal region, which had the highest summed outflow at the spike peak. In the RTLE group, the medial temporal pole had the highest outflow before, during, and after the spike peak, although the contralateral medial temporal pole and the ipsilateral rectus also reached their maximum value before the spike peak. In the LTLE group, the outflow from the medial temporal pole started declining after the spike peak, whereas the other drivers remained significant across the spike duration. In the RTLE group, the outflow from the medial temporal pole started decreasing slightly before the end of the spike. Analysis of the post–spike slow wave was not possible because slow waves were not present in all patients.

In all operated patients, the localization of the first key driver (temporal pole) was concordant with the epileptogenic zone estimated by resection volume (classical anterior temporal lobectomy).

Network pattern

A different network pattern between pairs of ROIs was observed in LTLE (Fig. 4A) and RTLE (Fig. 4B). The strongest connections in LTLE were within the ipsilateral temporal lobe and from these towards the ipsilateral frontal lobe. In contrast, the strongest connections in RTLE were found from the ipsilateral temporal to the contralateral temporal and bilateral frontal regions.

The laterality index showed a more lateralized network in LTLE than RTLE patients (respectively, mean 0.82 ± 0.18 and mean 0.44 ± 0.49; $p = 0.03$). The multivariate linear
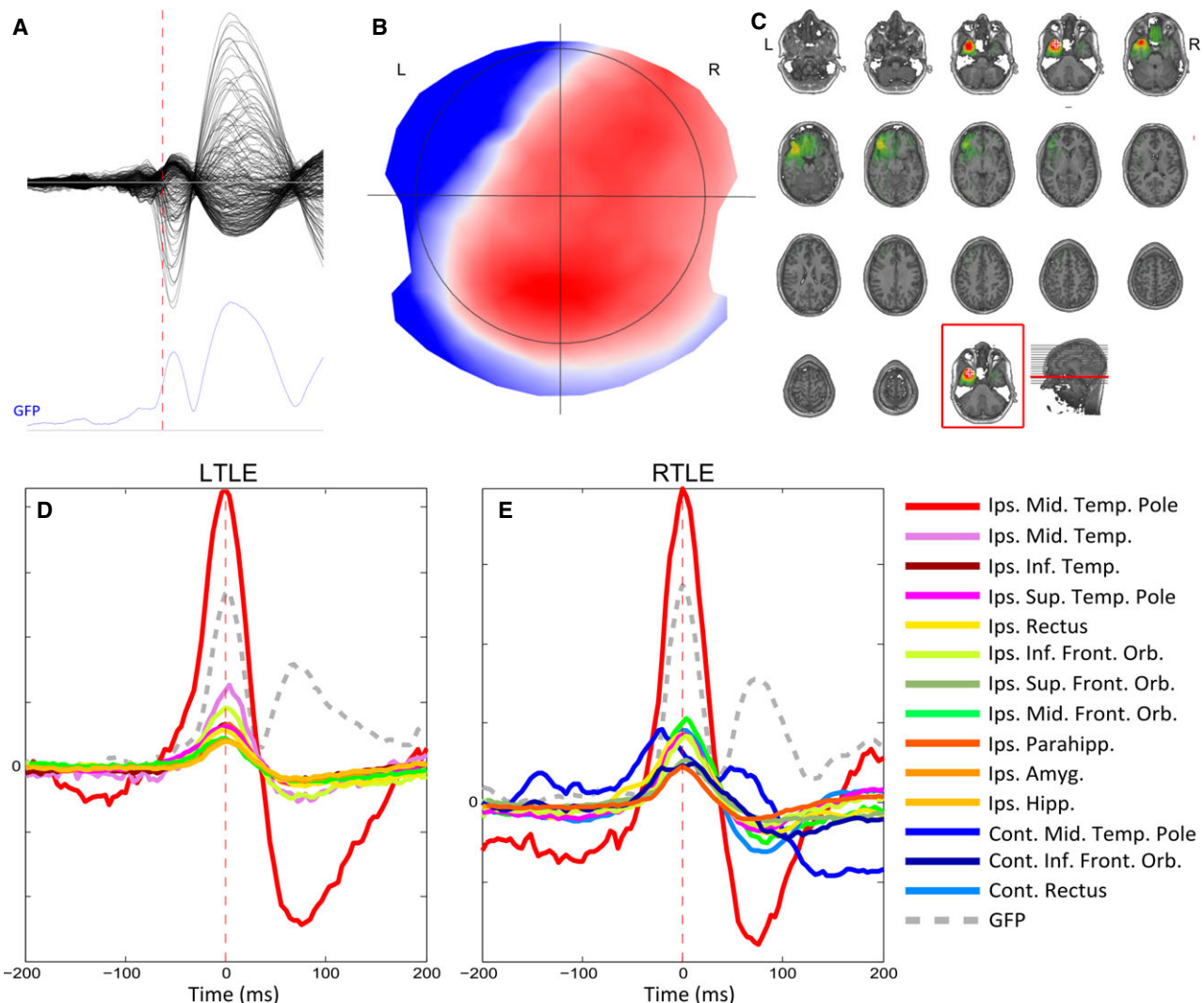
Figure 2.
Electrical source imaging (ESI) at the individual and group level (**A**) averaged spikes and global field power (GFP) for one individual patient. The red dashed line corresponds to the half rise of the spike. (**B**) Scalp electroencephalography (EEG) voltage map corresponding to the time point indicated in (**A**). (**C**) ESI at same time point. The maximum activity is localized in the medial temporal pole (**D**) ROIs activity across time for the LTLE group bottom and for the (**E**) RTLE group bottom. Note that the zero corresponds to the peak of the spike. The GFP is represented with a gray dashed line to display the temporal evolution of the global spike amplitude in the scalp EEG. Homologous regions are represented with the same color for both groups. Only the 10 highest activity regions are shown in each plot. Red/yellow/orange/green colors represent regions in the ipsilateral hemisphere, and blue colors represent regions in the contralateral hemisphere.
Epilepsia © ILAE

regression showed no statistically significant correlation between network laterality pattern and age or duration of disease.

Cognitive performances

In LTLE (Table 2), 50% (4/8) of the patients had deficits concordant with ipsilateral medial temporal dysfunction and 37.5% (3/8) had deficits suggesting frontal dysfunction. No patient showed a cognitive pattern of contralateral temporal deficit. In RTLE, 37.5% (3/8) of patients had ipsilateral temporal deficits, 50% (4/8) had contralateral temporal deficits and 75% (6/8) had frontal deficits. Significantly

more contralateral temporal deficits were found for RTLE (4/8) than LTLE (0/8) patients ($\chi^2 = 5.33$, p = 0.02).

DISCUSSION

We identified drivers and network patterns of interictal epileptic activity in TLE by combining EEG source imaging and time-varying Granger-causal modeling. The different network patterns found in LTLE and RTLE provide further evidence that those are not symmetrical entities. RTLE patients showed stronger connectivity targeting the contralateral hemisphere in comparison with LTLE patients, con-
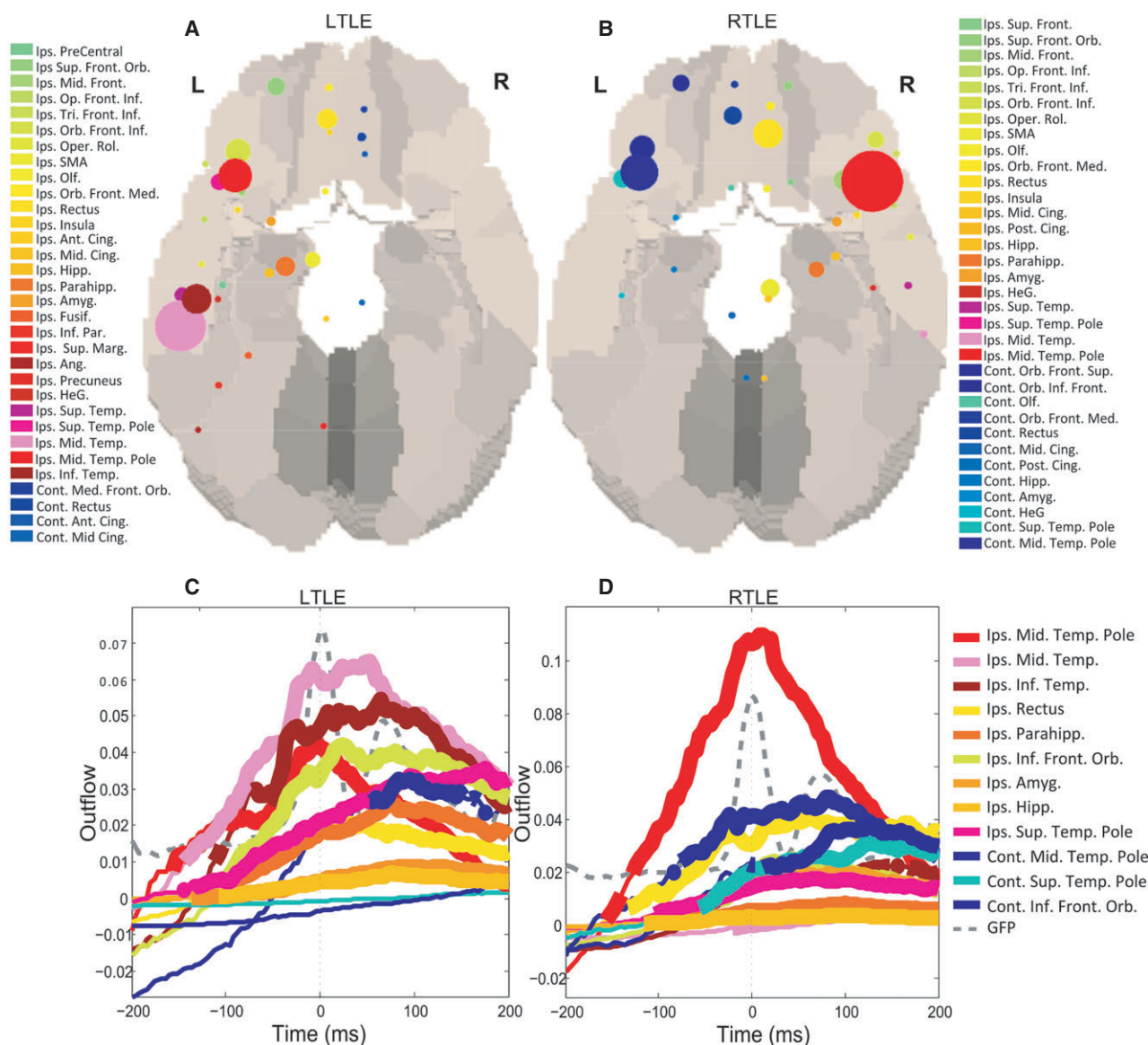
Figure 3.
Summed outflow related to the early spike (rising phase) for (**A**) the LTLE group and (**B**) the RTLE group. Only the regions in which at least half of the patients show a significant difference in the rising phase of the spike, compared to baseline, are displayed in the plots. Both plots have the same scales. The regions are projected on an axial slice across the temporal lobe for localization and the anatomic localization of the spheres should be interpreted according to their labels. Sphere radius is proportional to summed outflow of each ROI. Temporal evolution of the summed outflow for the (**C**) LTLE group and (**D**) RTLE group. These plots represent the difference between the summed outflow during spike vs baseline epochs. Thick lines represent time points with statistically significant difference during spike versus baseline epochs. The global field power (GFP, dashed gray line) indicates the temporal evolution of the spike itself. Red/yellow/orange/green colors represent regions in the ipsilateral hemisphere, and blue, regions in the contralateral hemisphere.
Epilepsia © ILAE

sistent with differences in neuropsychological impairments between the groups.

Spatial and temporal pattern of spike-related connectivity changes

The main driver in the early phase of the spike was in the ipsilateral anterior temporal lobe in both groups and suggests that EEG-directed connectivity can correctly identify the origin of epileptic discharges in this group of patients with invasive validation. However, we also observed other important secondary key drivers outside the ipsilateral temporal lobe, namely, in the frontal and contralateral areas. In LTLE, the key drivers were in the ipsilateral hemisphere, whereas in RTLE, the key drivers were in both ipsilateral and contralateral areas. This result was supported by larger current density shown by ESI in the contralateral ROIs in
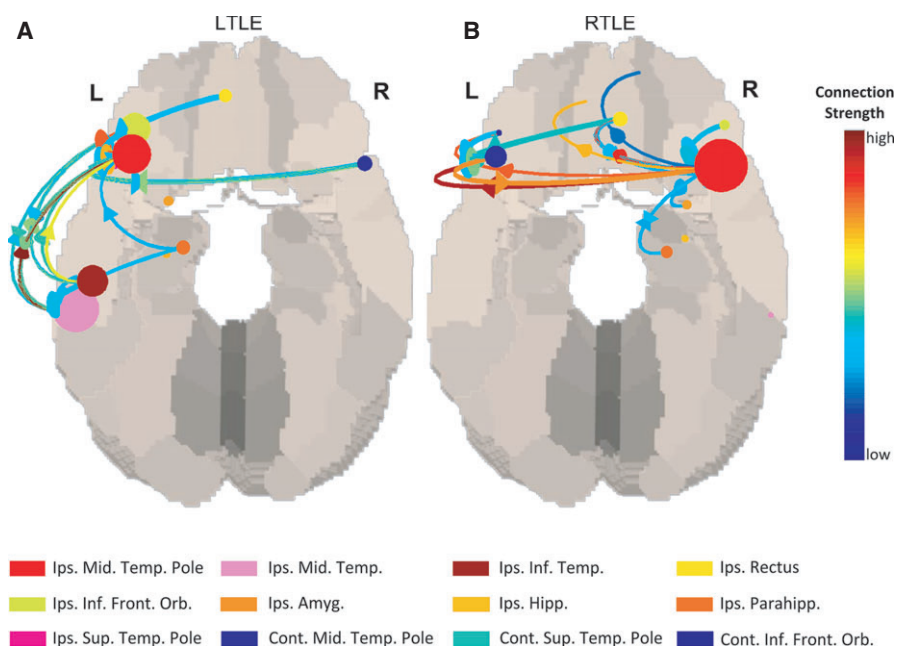
Figure 4.
Spike-related network patterns in (**A**) LTLE and (**B**) RTLE. Reciprocal significant connections are possible and are displayed. Note that the summed outflow is measured between each region and the whole brain, and thus individual connections from regions with lower summed outflow to regions with higher summed outflow are possible. The sphere radius is proportional to the summed outflow of each ROI. The strength of the connections is represented by the arrow color and the color scale on the right.
Epilepsia © ILAE

Table 2. Neuropsychological deficits in LTLE and RTLE patients		
	LTLE	RTLE
Ipsilateral temporal		
Medial	P2, P4, P5+, P8	P12, P14, P16
Middle/superior	P4	–
Inferior	–	–
Contralateral temporal		
Medial	–	P12+, P16
Middle/superior	–	P11, P15
Inferior	–	–
Frontal		
Medial	–	–
Middle/superior	P5, P4, P6	P10, P12, P14, P15, P16
Inferior	P6	P11+, P14
+: indicates severe deficit.		

LTLE compared to RTLE patients, confirming that these results are not a bias from the PDC algorithm. Moreover, not only the distribution of the main outflow regions but also the network pattern from the main driver was different in LTLE versus RTLE: the strongest connections from these main drivers were mainly toward the ipsilateral hemisphere in LTLE, whereas in RTLE they were mainly toward contralateral regions.

The ipsilateral temporal lobe was the earliest significant driver during the spike in both groups. The other identified key drivers were also early active, with high or even peak activity before the spike peak, concordant with a previous study showing that ESI of the rising phase of the spike is better at localizing epileptic activity, whereas the source at the spike peak can be contaminated by propagation.[28] Ipsilateral medial temporal structures (hippocampus and amygdala) were also identified as significant drivers, although with less summed outflow than the temporal pole. This confirms the notion that medial temporal structures can be "seen" by the scalp EEG even if simultaneous or propagated activity in lateral temporal areas dominates in strength.[30]

The characterization of the dynamics of interictal activity in the development of epileptic networks is important.[31] The emergence of spikes precedes the first seizure in animal models of epilepsy and may guide the development of aberrant neuronal circuits and the initiation of spontaneous seizures.[32] There is also evidence of spike-related cognitive impairments in epilepsy notably regarding memory maintenance and retrieval in the hippocampus of TLE patients.[11] Nevertheless, patterns of spike propagation may not be identical to seizure propagation and further ictal studies are needed.

Relevance of contralateral and extratemporal involvement

The existence of regions outside the ipsilateral temporal lobe with a high significant summed outflow supports previous evidence that impaired brain activity during

epileptic activity is not spatially restricted to the epileptogenic focus. Functional and structural studies showed that epileptic activity affect brain regions outside the seizure-onset zone, namely the contralateral temporal lobe,[10] the frontal lobe,[3,33,34] and other extratemporal regions.[35]

Indeed, connectivity studies have reported that normal physiologic networks can be disrupted in TLE.[8,9,35] As in MEG and intracranial EEG studies, we found disease-related connectivity increases in opposition to functional MRI (fMRI) studies reporting decrease of functional connectivity of hemodynamic signals.[8] This discrepancy between electrophysiologic and hemodynamic correlations is currently unexplained.

Functional and structural asymmetry of the two hemispheres has long been recognized.[36] We found more contralateral involvement in RTLE, in concordance with the neuropsychological assessment. Consistently, other studies demonstrated more contralateral hemisphere impairment in RTLE compared to LTLE using fMRI,[12] magnetic resonance spectroscopy (hippocampus),[13] and volumetry (subcortical structures).[14,37]

We observed that the strongest connection in the RTLE was from the ipsilateral to the contralateral medial temporal pole. Of interest, the reverse connection was also significantly increased during spikes, although weaker. The pathologic relevance of this observation is unknown. It could represent a compensatory mechanism[38] or alternatively, an altered feedback mechanism participating in the epileptogenicity, which can be increased by altered network characteristics in the absence of intrinsic excitability changes.[39]

Frontal regions were involved in both groups, concordant with studies showing propagation from medial temporal to frontal regions both in interictal spikes[40] or during invasively recorded seizures in TLE.[33] Particularly, the inferior frontal orbital region had a high summed outflow during the spike and was strongly connected with the temporal pole. In LTLE, the driving peak of this region occurred after the spike peak, suggesting a role of secondary driver of the epileptic activity, which is also supported by the strong outflow from the temporal pole to the inferior frontal orbital region (Fig. 4A). In RTLE, this inferior frontal orbital involvement occurred earlier and in a more bilateral way (Fig. 4B). These findings could be related to the important role of the pyriform cortex in epileptic networks, as demonstrated by human positron emission tomography (PET) and fMRI studies.[41] There is convincing evidence that basal frontal activity can be detected by scalp electrodes[42] and the ROI-based approach could explain the imperfect match between our results and the localization of the pyriform cortex.

Frontal cognitive deficits in TLE have been linked to the high interconnectivity between frontal and temporal regions.[34] Indeed, frontotemporal regions underlie working memory and executive functions, which are often impaired in TLE.[3] In our patients, the connectivity increase between the temporal and the frontal lobes was concordant with frontal cognitive deficits, predominantly in RTLE.

Methodologic considerations

The measure of brain connectivity using EEG source signals avoids pitfalls encountered with surface signals analysis. First, the volume conduction problem: all electrodes measure the combined activity of several source.[43] Volume conduction is also present in source signals but zero-lag correlations do not influence PDC results.[44] Second, the reference problem: scalp EEG signal and their analysis are heavily influenced by the reference signal, whereas the source activity is reference free.[24] Third, ESI based on high-density EEG and individual brain anatomy reliably localizes interictal activity including in medial temporal and basal frontal regions, as established by large invasively validated clinical studies.[20,30,42] Moreover, ESI of interictal spikes is a reliable surrogate marker of the seizure-onset zone.[20] Given that ESI might have difficulty distinguishing between temporopolar and strictly medial temporal sources (amygdala, anterior hippocampus), the strongest driving seen in the temporal pole should be considered as generated by the anteromedial temporal lobe rather than strictly the temporal pole. Nevertheless, even if weaker in strength, ESI and connectivity analysis seem able to discriminate medial and lateral temporal structures and support the strong interconnections between these areas in TLE.[8]

Our results highlight statistical differences between interictal spikes and baseline periods and not baseline abnormalities in patients versus controls. Future studies should investigate alteration of baseline EEG activity in TLE patients. Finally, connectivity changes during post–spike slow waves were not systematically observed and therefore not studied.

We subjectively selected regions that presented significant results in the majority of the patients in order to display commonalities within groups. This compensates for multiple statistical comparisons that were not strictly accounted for. The obtained findings are concordant with the invasive findings and neuropsychology testing.

We focused only on the frequency of maximal spectral power (observed in the theta band) because we considered frequencies with high spectral power as potential large drivers of the network. However, it is possible that other frequencies are important in spike generation and propagation, for example, high frequency oscillations (HFO),[45] and these should be investigated in future work. Indeed, it has been repeatedly reported that epileptic spike discharges in the hippocampus are accompanied by HFO in the 200–500 Hz range.[46] These HFO can also be observed in human intracranial recordings and are supposed to reflect fields of hypersynchronized action potentials.[47] Consequently one could argue that information transfer is carried by the HFO rather than the dominant frequency of the local field potential considered in this study. However, HFO are only rarely

recorded with scalp EEG,[48] and higher sampling rates than those used in our recordings are needed. Therefore, scalp EEG spikes are dominated by local field potentials that represent postsynaptic potentials with dominant frequency in the theta range. Further studies are needed, particularly using multisite intracranial recordings, to study information transfer in the HFO frequency range.

The group connectivity differences were not likely caused by different etiologies across groups, as most patients had hippocampal sclerosis, whereas the others had other medial or polar temporal lesions, and we saw no consistent differences in individual connectivity maps between hippocampal sclerosis patients and other etiologies. Likewise, age of onset and disease duration were not different between groups.

Our semi-quantitative cognitive scores accounted for effects of attention and education level that might confound individual specific quantitative scores. The connectivity pattern should be correlated with more detailed neuropsychological profiles in a larger population to confirm the association between cognitive performances and network patterns.

Conclusion

We identified the major drivers of interictal epileptic activity in RTLE and LTLE, concordant with invasive validation. Moreover, we found different patterns of time-varying connectivity in LTLE and RTLE, suggesting that these are not symmetrical entities, in line with our neuropsychological results. This enhanced characterization of dynamic connectivity patterns could better explain cognitive deficits and help the management of epilepsy surgery candidates.

Acknowledgments

Disclosure

None of the authors has any conflict of interest to disclose. We confirm that we have read the Journal's position on issues involved in ethical publication and affirm that this report is consistent with those guidelines.

References

1. Richardson MP. Large scale brain models of epilepsy: dynamics meets connectomics. *J Neurol Neurosurg Psychiatry* 2012;83:1238–1248.
2. de Tisi J, Bell GS, Peacock JL, et al. The long-term outcome of adult epilepsy surgery, patterns of seizure remission, and relapse: a cohort study. *Lancet* 2011;378:1388–1395.
3. Stretton J, Thompson PJ. Frontal lobe function in temporal lobe epilepsy. *Epilepsy Res* 2012;98:1–13.
4. Oyegbile TO, Dow C, Jones J, et al. The nature and course of neuropsychological morbidity in chronic temporal lobe epilepsy. *Neurology* 2004;62:1736–1742.
5. Dai Y, Zhang W, Dickens DL, et al. Source connectivity analysis from MEG and its application to epilepsy source localization. *Brain Topogr* 2012;25:157–166.
6. van Mierlo P, Carrette E, Hallez H, et al. Accurate epileptogenic focus localization through time-variant functional connectivity analysis of intracranial electroencephalographic signals. *Neuroimage* 2011;56:1122–1133.
7. van Mierlo P, Carrette E, Hallez H, et al. Ictal-onset localization through connectivity analysis of intracranial EEG signals in patients with refractory epilepsy. *Epilepsia* 2013;54:1409–1418.
8. Bettus G, Ranjeva JP, Wendling F, et al. Interictal functional connectivity of human epileptic networks assessed by intracerebral EEG and BOLD signal fluctuations. *PLoS ONE* 2011;6:e20071.
9. Wilke C, van Drongelen W, Kohrman M, et al. Identification of epileptogenic foci from causal analysis of ECoG interictal spike activity. *Clin Neurophysiol* 2009;120:1449–1456.
10. Seidenberg M, Kelly KG, Parrish J, et al. Ipsilateral and contralateral MRI volumetric abnormalities in chronic unilateral temporal lobe epilepsy and their clinical correlates. *Epilepsia* 2005;46:420–430.
11. Holmes GL, Lenck-Santini PP. Role of interictal epileptiform abnormalities in cognitive impairment. *Epilepsy Behav* 2006;8:504–515.
12. Dupont S, Samson Y, Van de Moortele PF, et al. Bilateral hemispheric alteration of memory processes in right medial temporal lobe epilepsy. *J Neurol Neurosurg Psychiatry* 2002;73:478–485.
13. Zubler F, Seeck M, Landis T, et al. Contralateral medial temporal lobe damage in right but not left temporal lobe epilepsy: a (1)H magnetic resonance spectroscopy study. *J Neurol Neurosurg Psychiatry* 2003;74:1240–1244.
14. Pail M, Brazdil M, Marecek R, et al. An optimized voxel-based morphometric study of gray matter changes in patients with left-sided and right-sided mesial temporal lobe epilepsy and hippocampal sclerosis (MTLE/HS). *Epilepsia* 2010;51:511–518.
15. Baccala LA, Sameshima K. Partial directed coherence: a new concept in neural structure determination. *Biol Cybern* 2001;84:463–474.
16. Plomp G, Quairiaux C, Michel CM, et al. The physiological plausibility of time-varying Granger-causal modeling: normalization and weighting by spectral power. *Neuroimage* 2014;101:547–554.
17. Astolfi L, Cincotti F, Mattia D, et al. Tracking the time-varying cortical connectivity patterns by adaptive multivariate estimators. *IEEE Trans Biomed Eng* 2008;55:902–913.
18. Adhikari BM, Epstein CM, Dhamala M. Localizing epileptic seizure onsets with Granger causality. *Phys Rev E Stat Nonlin Soft Matter Phys* 2013;88:030701.
19. Birot G, Spinelli L, Vulliémoz S, et al. Head model and electrical source imaging: a study of 38 epileptic patients. *Neuroimage Clin* 5:77–83.
20. Megevand P, Spinelli L, Genetti M, et al. Electric source imaging of interictal activity accurately localises the seizure onset zone. *J Neurol Neurosurg Psychiatry* 2014;85:38–43.
21. Grave de Peralta Menendez R, Murray MM, Michel CM, et al. Electrical neuroimaging based on biophysical constraints. *Neuroimage* 2004;21:527–539.
22. Tzourio-Mazoyer N, Landeau B, Papathanassiou D, et al. Automated anatomical labeling of activations in SPM using a macroscopic anatomical parcellation of the MNI MRI single-subject brain. *Neuroimage* 2002;15:273–289.
23. Stockwell RG, Mansinha L, Lowe RP. Localization of the complex spectrum: the S Transform. *IEEE Trans Signal Process* 1996;44:998–1001.
24. Koenig T, Pascual-Marqui RD Multichannel frequency and time-frequency analysis. In Michel CMK, Koenig T, Brandeis D, Gianotti LRR, Wackermann J (Eds) *Electrical neuroimaging,* Cambridge: Cambridge University Press, 145–168.
25. Hesse W, Moller E, Arnold M, et al. The use of time-variant EEG Granger causality for inspecting directed interdependencies of neural assemblies. *J Neurosci Methods* 2003;124:27–44.

26. Astolfi L, Cincotti F, Mattia D, et al. Assessing cortical functional connectivity by partial directed coherence: simulations and application to real data. *IEEE Trans Biomed Eng* 2006;53:1802–1812.

27. Chan HL, Tsai YT, Wang YC, et al. Partial directed coherence analysis of intracranial neural spikes in epilepsy patients. *Conf Proc IEEE Eng Med Biol Soc* 2012;2012:5174–5177.

28. Lantz G, Spinelli L, Seeck M, et al. Propagation of interictal epileptiform activity can lead to erroneous source localizations: a 128-channel EEG mapping study. *J Clin Neurophysiol* 2003;20:311–319.

29. He B, Dai Y, Astolfi L, et al. eConnectome: a MATLAB toolbox for mapping and imaging of brain functional connectivity. *J Neurosci Methods* 2011;195:261–269.

30. Brodbeck V, Spinelli L, Lascano AM, et al. Electroencephalographic source imaging: a prospective study of 152 operated epileptic patients. *Brain* 2011;134:2887–2897.

31. Stefan H, Lopes da Silva FH. Epileptic neuronal networks: methods of identification and clinical relevance. *Front Neurol* 2013;4:8.

32. Staley KJ, Dudek FE. Interictal spikes and epileptogenesis. *Epilepsy Curr* 2006;6:199–202.

33. Lieb JP, Dasheiff RM, Engel J Jr. Role of the frontal lobes in the propagation of mesial temporal lobe seizures. *Epilepsia* 1991;32:822–837.

34. O'Muircheartaigh J, Richardson MP. Epilepsy and the frontal lobes. *Cortex* 2012;48:144–155.

35. Cataldi M, Avoli M, de Villers-Sidani E. Resting state networks in temporal lobe epilepsy. *Epilepsia* 2013;54:2048–2059.

36. Cohen BD, Noblin CD, Silverman AJ, et al. Functional asymmetry of the human brain. *Science* 1968;162:475–477.

37. Seeck M, Lazeyras F, Murphy K, et al. Psychosocial functioning in chronic epilepsy: relation to hippocampal volume and histopathological findings. *Epileptic Disord* 1999;1:179–185.

38. Bettus G, Guedj E, Joyeux F, et al. Decreased basal fMRI functional connectivity in epileptogenic networks and contralateral compensatory mechanisms. *Hum Brain Mapp* 2009;30:1580–1591.

39. Terry JR, Benjamin O, Richardson MP. Seizure generation: the role of nodes and networks. *Epilepsia* 2012;53:e166–e169.

40. Emerson RG, Turner CA, Pedley TA, et al. Propagation patterns of temporal spikes. *Electroencephalogr Clin Neurophysiol* 1995;94:338–348.

41. Laufs H, Richardson MP, Salek-Haddadi A, et al. Converging PET and fMRI evidence for a common area involved in human focal epilepsies. *Neurology* 2011;77:904–910.

42. Ramantani G, Dumpelmann M, Koessler L, et al. Simultaneous subdural and scalp EEG correlates of frontal lobe epileptic sources. *Epilepsia* 2014;55:278–288.

43. Schoffelen JM, Gross J. Source connectivity analysis with MEG and EEG. *Hum Brain Mapp* 2009;30:1857–1865.

44. Haufe S, Nikulin VV, Muller KR, et al. A critical assessment of connectivity measures for EEG data: a simulation study. *Neuroimage* 2013;64:120–133.

45. Jacobs J, LeVan P, Chander R, et al. Interictal high-frequency oscillations (80–500 Hz) are an indicator of seizure onset areas independent of spikes in the human epileptic brain. *Epilepsia* 2008;49:1893–1907.

46. Bragin A, Mody I, Wilson CL, et al. Local generation of fast ripples in epileptic brain. *J Neurosci* 2002;22:2012–2021.

47. Jefferys JG, Menendez de la Prida L, Wendling F, et al. Mechanisms of physiological and epileptic HFO generation. *Prog Neurobiol* 2012;98:250–264.

48. Zelmann R, Lina JM, Schulze-Bonhage A, et al. Scalp EEG is not a blur: it can see high frequency oscillations although their generators are small. *Brain Topogr* 2014;27:683–704.

Supporting Information

Additional Supporting Information may be found in the online version of this article:

Table S1. Regional brain dysfunction based on the interpretation of neuropsychological assessment.